Proceedings of the European Conference Physics of Magnetism, Poznań 2017

Electronic Structure of Th_7Ru_3

M. Sahakyan* and V.H. Tran
Institute of Low Temperature and Structure Research, Polish Academy of Sciences,
PO. Box 1410, 50-422 Wrocław, Poland

We report the results of scalar and fully relativistic electronic structure calculations for nonsuperconducting Th_7Ru_3, using the full-potential linearized-muffin-thin-orbital and full-potential linearized augmented-plane wave methods. The obtained data, including electronic band structures, density of states, Fermi surfaces and electron localization function, reveal the presence of anisotropic spin-orbit coupling but its strength, exposed by splitting energies of the order of 10–40 meV, is much weaker as compared to those of Th_7Fe_3 or Th_7Co_3 superconductors. Moreover, the lack of Van Hove singularity near the Fermi level underscores a key point of the non-occurrence of superconductivity in the studied compound.

DOI: 10.12693/APhysPolA.133.751
PACS/topics: 71.15.Mb, 71.15.Rf, 71.18.+y, 71.20.–b, 74.20.Mn,74.20.Rp

1. Introduction

The non-relativistic Schrödinger equation provides the spin degenerate energetic levels of atoms in solid state physics. In order to eliminate this degeneration, the spin-orbit (SO) interaction should be treated as a relativistic correction [1]. In crystals, the electric field is given by the gradient of crystal potential, which produces SO field and describes the interactions of spin angular momentum and orbital momentum [2]. The lack of inversion symmetry in crystals introduces a special form of SO coupling, which is called anti-symmetric spin-orbit coupling (ASOC) [3, 4]. Concerning the quantum wells with the broken inversion symmetry along the growth direction, Vasko [5], Bychkov and Rashba [6] proposed that the interlayer electric field $\boldsymbol{E} = E_z \cdot \hat{z}$ results in a SO coupling of the form $\hat{H}_{\mathrm{SO}} = \alpha_R(\hat{z} \cdot \boldsymbol{p}) \cdot \hat{\sigma}$ where α_R is known as the Rashba parameter. The magnitude of the α_R depends on the electric field, atomic weight and atomic shells involved [7]. This $\hat{H}_{\mathrm{SO}}$ as an additional part of Hamiltonian, provides a spin splitting in the degenerate energy bands, and also splitting Fermi surface into two sheets. When ΔE^{SO} (the magnitude of SO splitting) is sufficiently large in respect of the superconducting gap, then the superconductors can exhibit an unconventional pairing symmetry, such as in the case of $CePt_3Si$ [8], $CeRuSi_3$ [9], UIr [10], $LaNiC_2$ [11], Li_2Pt_3B [12], Re_6Zr [13], or can affect exotic behavior relating to the superconducting gaps, e.g. in Th_7Co_3 [14], Th_7Fe_3 [15]. In this paper, we present the results of the electronic structure calculation of the non-centrosymmetric Th_7Ru_3 compound by the Full-Potential Linearized Muffin Tin Orbital (FP-LMTO) and Full-Potential Linearized Augmented-Plane Wave (FP-LAPW) methods. We discuss different impacts of ASOC effect on the physical properties of the studied compound. It is to be recalled that in contrast to superconducting Th_7T_3 with T = Co, Fe, Rh, Os, Ir, Ni, discovered by Matthias [16], Th_7Ru_3 does not show superconductivity at all.

*corresponding author; e-mail: m.sahakyan@int.pan.wroc.pl

2. Computational results

Th_7Ru_3 crystallizes in hexagonal-type structure with the space group $P6_3mc$. The lattice parameters of Th_7Ru_3 studied in this work are taken to be $a = b = 0.9996$ nm and $c = 0.6302$ nm. The thorium atoms in the unit cell are characterized by the three atomic positions with Th_1, Th_2 located at $6c$ positions and Th_3 at $2b$ position, while ruthenium atoms occupy one position ($6c$) [16]. The calculations based on the FP-LMTO method have been performed with the LMTART computational code [17, 18]. The atomic sphere radii of the atoms have been found self-consistently as: $R_{Th_1} = 2.159$, $R_{Th_2} = 2.355$, $R_{Th_3} = 1.976$ a.u., and $R_{Fe} = 1.972$ a.u.. A total number of 112896 fast Fourier transform (FFT) points have been generated, with the $(56, 56, 36)$ divisions. In the case of FP-LAPW method we have utilized the high precision all-electron ELK code [19]. As the exchange-correlation energy, the local density approximation (LDA) is used [20, 21] with the generalized gradient approximation (GGA) [22]. The electronic charge density convergence was achieved by employing the tetrahedron method of $\boldsymbol{k}$-integration, and by using $(8, 8, 12)$ $\boldsymbol{k}$-mesh in the irreducible wedge of Brillouin zone (BZ).

The electronic band structures of Th_7Ru_3 along the high-symmetry lines of the BZ obtained with the FP-LMTO and FP-LAPW methods are similar. Therefore, in Fig. 1, we show only the FP-LMTO results. Using the scaler relativistic (SR) treatment, we get three degenerated bands (blue color) crossing the Fermi level. However, when the fully relativistic (FR) treatment including spin-orbit interaction was taken into account, asymmetric band splitting (red color) appears as due to the ASOC effect. It is seen as one of important results of our studies the splitting is anisotropic in the whole range of particle

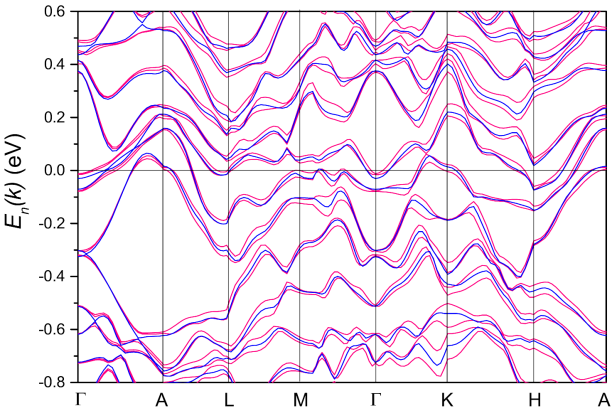

Fig. 1. The electronic band structures of Th_7Ru_3, calculated by SR (blue color) and FR (red color) approximations.

energy spectrum and along all directions of the reciprocal wave vector $|\boldsymbol{k}|$. It is clear that the splitting is small in the direction $\Gamma - A$ as compared to the other high symmetry directions. The feature is very reminiscent of the behaviour of Th_7Co_3 and Th_7Fe_3 superconductors [14,15], and supports the noncentrosymmetric nature of the studied Th_7Ru_3 compound. A comparison of SR and FR data divulges the spin splitting energy of about $10 - 40$ meV, which is by $2 - 3$ times smaller compared to Th_7Co_3 and Th_7Fe_3. Displacement of the energy bands is also very small ($3 - 30$ meV), implying that the influence of SO coupling is essentially weak.

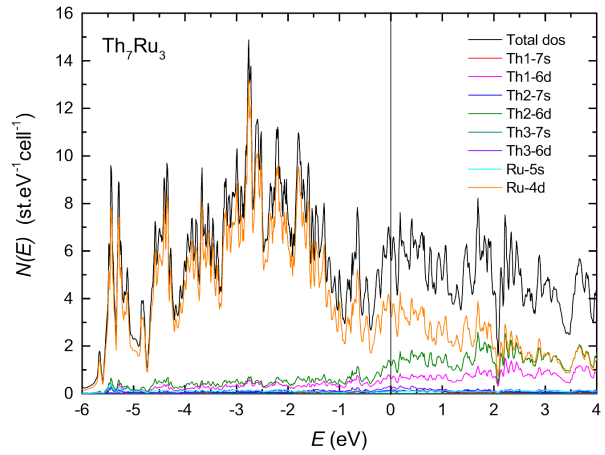

Fig. 2. The total and partial DOS of Th_7Ru_3.

In Fig. 2, we show the total and partial (PDOS) DOS's of Th_7Ru_3 calculated within the FR approach using the FP-LMTO method. Since the Th atoms occupy in the three atomic positions, they contribute differently to the total DOS. The PDOS of Th_2-6d is ~ 2 times bigger than Th_1-6d, while the PDOS of Th_3-6d is smaller by a factor of ~ 4. We observe that the electrons of the orbitals Ru-4d and Th-6d play the main role in the electronic DOS structure. However, the dominant role bellow the Fermi level is due to Ru-4d electrons, where they display the peak-structured features. It is known that the superconducting properties are manifested in DOS by the presence of so-called Van Hove peak, which is located very close to the Fermi level. Apparently, the peak-structured DOS of Th_7Ru_3 centered at ~ -2.8 eV is much deeper as compared to those of Fe-, Co-based superconductors of about –0.7 eV [15, 14]. Therefore we may conclude that the absence of the Van Hove singularities in DOS structure accords well with the lack of the superconductivity in Th_7Ru_3.

We estimated the total DOS value at the Fermi level to be 5.61 st/(eVcell) corresponding $N(E_F) = 11.22$ st.(eV.f.u.)$^{-1}$, for both spin directions. The PDOS contributions of the Ru-4d and Th-6d orbitals to $N(E_F)$ are 3.25 and 2.1 st.(eV/cell), respectively.

Putting the DOS value at E_F to the equation:

$$\gamma_{theo} = \frac{1}{3}\pi^2 k_B N_A N(E_F), \qquad (1)$$

where k_B is the Boltzmann constant and N_A is the Avogadro number, we obtained the theoretical Sommerfeld coefficient $\gamma_{theo} = 26.41$ mJ/molK^2, which is in good agreement with the the experimental value $\gamma_{exp} = 36.3$ mJ/molK^2 [23]. It is emphasized both the $N(E_F$ and γ_{theo} values of Th_7Ru_3 are considerably smaller than corresponding quantities of Th_7Fe_3 ($N(E_F) = 16.7$ st.(eV f.u.)$^{-1}$, $\gamma_{theo} = 39.31$ mJ/molK^2) [15] and Th_7Co_3 ($N(E_F) = 15$ st. (eVf.u.)$^{-1}$, $\gamma_{theo} = 35.3$ mJ/molK^2) [14] superconductors.

The FP-LAPW calculation furnished similar total and partial DOS as those from the FP-LMTO. In addition, we attained a new information on the density of states coming from the overlapping regions. It turns that the interstitial DOS (not shown here) constitutes as much as about 50 % of the total DOS.

The next impact of noncentrosymmetric nature on the electronic properties of Th_7Ru_3 compound is revealed from the Fermi surface topologies, which are presented in Fig. 3. The SR (shown by the green color) and FR (in red color) calculations were performed for the energy bands of the number 48–50. In the upper panel of Fig. 3, we show the FS formed by spin-down states, while in the lower panel those coming from the spin-up states. It is seen first of all that the shapes of the FS along the high-symmetry lines Σ, Λ and P differ from each other. This finding points to anisotropic structures of the FS. It is also worthwhile to underline that at some symmetry points, the Fermi surface topologies accomplished by these two approaches are different. This could reasonably be understood as due to the anisotropic Fermi surface splitting in the $\boldsymbol{k}$-space, emerged by the influence of ASOC. Based on the FS data, we can prove also that the splitting energy in Th_7Ru_3 is smaller than in Th_7Fe_3 [15], which again supports a weaker effect of ASOC.

Figure 4a–c show the Electron Localization Function (ELF) [24] 3D-representation for the 001, 010 and 110-sections through the Th and Ru atoms. It appears that

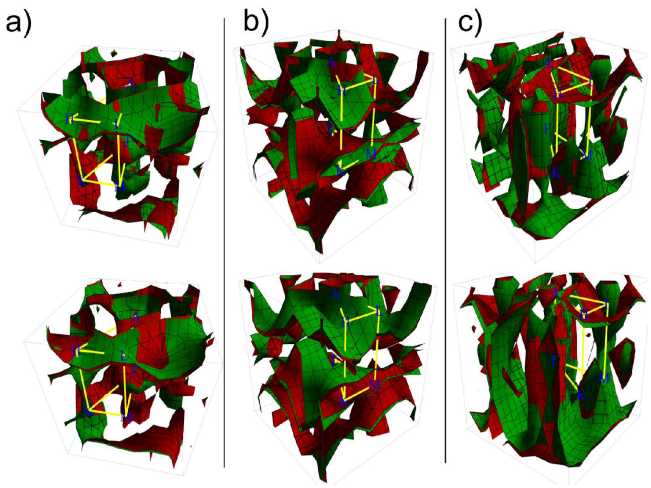

Fig. 3. The FS topologies of Th_7Ru_3, calculated by the SR (green color) and FR (red color) approximations. The FS formed by the spin-down states are presented in the upper panel, while these formed by spin-up states in the lower panel.

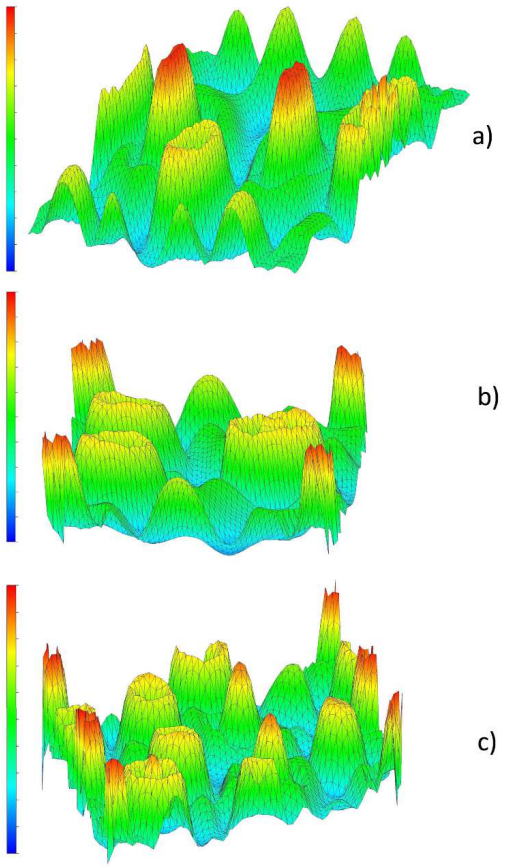

Fig. 4. 3D ELF representation of a) the 001-, b) 010- and c) 110- surfaces of Th_7Ru_3. The ELF values are bound between 0 (blue color) and 1 (red color).

there are topological differences between regions at Th and at Ru atoms. The ELF distribution around Ru is characterized by peaked maxima and almost spherically symmetric.

Very high values of ELF (about 0.9) at the maxima indicate that the electrons are strongly paired, thus they are attractors [25]. This situation is in contrast to those of Th atoms, where ELF exhibits broader structures with anisotropic shapes resembling volcano holes. A striking fact is also that inside the "volcano holes" there exists sure peak, which results in the formation of a valley separating the spheric core region and external wall. The ELF values of the external wall of approximately 0.75 are quite high. This finding implies the presence of covalent bonds nearby the core regions of the Th atoms too. Remarkably, we may distinguish another ELF maxima, which are not associated with any core region of constituted atoms. The ELF values at these maxima are approaching 0.5, suggesting region of delocalized electrons.

3. Summary

We have performed first-principle calculations of the EBS, DOS, FS and ELF for noncentrosymmetric Th_7Ru_3 compound, using FP-LMTO and FP-LAPW methods. From the FR approach, it follows the existence of the asymmetric spin-orbit coupling (ASOC) in the systems with the lack of the inversion symmetry, and this causes the spin splitting in both energy bands and FS topologies. However, in Th_7Ru_3 the impact of ASOC is weak ($10-40$ mev) in comparison to those of Th_7Fe_3 and Th_7Co_3, for which the splitting energy is $\sim 2-3$ times larger. We believe that the strength of ASOC determines non- or superconducting properties of Th_7T_3 (T = Ru, Fe, Co). The DOS of Th_7Ru_3 does not exhibit Van Hove singularity, being consistent with nonsuperconducting property of the studied compound.

We have shown that the main contribution to total DOS at the Fermi level comes from the Ru-4*d* with $N(E_F) = 3.25$ st.eV^{-1}cell^{-1} and Th–6d $N(E_F) = 2.1$ st.eV^{-1}cell^{-1} orbital electrons. We conclude that the valence bands coming from Ru-4*d* orbitals form the peak-structured features in the DOS, caused by the Ru-4*d* valence bands centered at –2.8 eV. This feature together with low $N(E_F)$ are evidences that the Ru-4*d* states are more localized than Fe(or Co) in Th_7(Fe, Co)$_3$.

We have calculated ELF and analysed the bonding nature in Th_7Ru_3. The topological examination of the ELF revealed anisotropic distributions of electron pair density, whereas comparison of ELF values the coexistence of covalent and metallic bondings in the studied material.

Acknowledgments

The work was supported by the National Science Centre (Poland) under the Grant No. 2016/21/B/ST3/01366.

References

[1] C. Møller, *The Theory Of Relativity*, Oxford at the Claredon Press, London 1952.

[2] L.H. Thomas, *Nature (London)* **117**, 514(1926).

[3] E. Rashba, *Sov. Phys. Solid State* **2**, 1109 (1960).

[4] L. Gorkov, E. Rashba, *Phys. Rev. Lett.* **87**, 037004 (2001).

[5] F.T. Vasko, *P. Zh. Eksp. Teor. Fiz.* **30**, 574 (1979).

[6] Y. Bychkov, E. Rashba, *P. Zh. Eksp. Teor. Fiz.* **39**, 66 (1984).

[7] L. Petersen, P. Hedegard, *Surf. Sci.* **459**, 49 (2000).

[8] E. Bauer, G. Hilscher, H. Michor, C. Paul, E. Scheidt, A. Gribanov, Y. Seropegin, H. Noel, M. Sigrist, P. Rogl, *Phys. Rev. Lett.* **92**, 027003 (2004).

[9] N. Kimura, K. Ito, K. Saitoh, Y. Umeda, H. Aoki, T. Terashima, *Phys. Rev. Lett.* **95**, 247004 (2005).

[10] T. Akazawa, H. Hidaka, H. Kotegawa, T. Kobayashi, T. Fujiwara, E. Yamamoto, Y. Haga, R. Settai, Y. Ōnuki, *J. Phys. Soc. Japn* **73**, 3129 (2004).

[11] K.-W. Lee, W.E. Pickett, *Phys. Rev. B* **72**, 174505 (2005).

[12] A. Hillier, J. Quintanilla, R. Cywinski, *Phys. Rev. Lett.* **102**, 117007 (2009).

[13] R. Singh, A. Hillier, B. Mazidian, J. Quintanilla, F. Annett, D.M. Paul, G. Balakrishnan, M. Lees, *Phys. Rev. Lett.* **112**, 107002 (2014).

[14] M. Sahakyan, V.H. Tran, *J. Phys.: Condens. Matter* **28**, 205701 (2016).

[15] M. Sahakyan, V.H. Tran, *Philos. Mag.* **42**, 957 (2017).

[16] B.B. Matthias, V. Compton, E. Corenzwit, *J. Phys. and Chem. Solids* **19**, 130 (1961).

[17] S.Y. Savrasov, D.Y. Savrasov, *Phys. Rev. B* **46**, 12181 (1992).

[18] S.Y. Savrasov, *Phys. Rev. B* **54**, 16470 (1996).

[19] K. Dewhurst, et al., *The Elk FP-LAPW code*, Version 4.3.6.

[20] J.P. Perdew, W. Yue, *Phys. Rev. B* **33**, 8800 (1986).

[21] J.P. Perdew, Y. Wang, *Phys. Rev. B* **45**, 13244 (1992).

[22] J.P. Perdew, K. Burke, Y. Wang, *Phys. Rev. B* **54**, 16533 (1996).

[23] J. Smith, J. Lashley, H. Volz, R. Fisher, P. Riseborough, *Phil. Mag.* **88**, 2847 (2008).

[24] F.R. Wagner, *Electron localizability: chemical bonding analysis in direct and momentum space*, Max-Planck Institut für Chemische Physik fester Stoffe 2002.

[25] A. Savin, R. Nesper, S. Wengert, T.F. Fässler, *Angew. Chem. Int. Ed. Engl.* **36**, 1808 (1997).